GENETICS, 2022, 222(2), iyac119
https://doi.org/10.1093/genetics/iyac119
Advance Access Publication Date: 10 August 2022
Investigation

Cytological heterogeneity of heterochromatin among 10 sequenced *Drosophila* species

Marcella Marchetti ,[1] Lucia Piacentini ,[1] Maria Francesca Berloco ,[2] Assunta Maria Casale ,[1] Ugo Cappucci ,[1] Sergio Pimpinelli ,[1,*] Laura Fanti [1,*]

[1]Istituto Pasteur Italia and Dipartimento di Biologia e Biotecnologie "Charles Darwin", "Sapienza" University of Rome, 00185 Rome, Italy,
[2]Dipartimento di Biologia, Università degli Studi di Bari "Aldo Moro", 70121 Bari, Italy

*Corresponding author: Istituto Pasteur Italia and Dipartimento di Biologia e Biotecnologie "Charles Darwin", "Sapienza" University of Rome, 00185 Rome, Italy. Email: laura.fanti@uniroma1.it, sergio.pimpinelli@uniroma.it

Abstract

In *Drosophila* chromosomal rearrangements can be maintained and are associated with karyotypic variability among populations from different geographic localities. The abundance of variability in gene arrangements among chromosomal arms is even greater when comparing more distantly related species and the study of these chromosomal changes has provided insights into the evolutionary history of species in the genus. In addition, the sequencing of genomes of several *Drosophila* species has offered the opportunity to establish the global pattern of genomic evolution, at both genetic and chromosomal level. The combined approaches of comparative analysis of syntenic blocks and direct physical maps on polytene chromosomes have elucidated changes in the orientation of genomic sequences and the difference between heterochromatic and euchromatic regions. Unfortunately, the centromeric heterochromatic regions cannot be studied using the cytological maps of polytene chromosomes because they are underreplicated and therefore reside in the chromocenter. In *Drosophila melanogaster*, a cytological map of the heterochromatin has been elaborated using mitotic chromosomes from larval neuroblasts. In the current work, we have expanded on that mapping by producing cytological maps of the mitotic heterochromatin in an additional 10 sequenced *Drosophila* species. These maps highlight 2 apparently different paths, for the evolution of the pericentric heterochromatin between the subgenera Sophophora and Drosophila. One path leads toward a progressive complexity of the pericentric heterochromatin (Sophophora) and the other toward a progressive simplification (Drosophila). These maps are also useful for a better understanding how karyotypes have been altered by chromosome arm reshuffling during evolution.

Keywords: heterochromatin; evolution; *Drosophila* species

Introduction

Within an organism, genes are arranged in a linear order along the chromosomes. However, just as mutations change the structure of genes, chromosomal rearrangements occur that change the order of genes. Once these rearrangements occur, they can be maintained and cause karyotypic variability both within and among populations from different geographic localities. The study of these chromosomal changes has allowed an assessment of the evolutionary history of multiple species (Ruiz and Fontdevila 1985; Yogeeswaran *et al.* 2005; Fuller *et al.* 2018; Auvinet *et al.* 2020; Franchini *et al.* 2020).

The genus *Drosophila* has a long history in the study of chromosomal arrangements due in large part to the presence of polytene chromosomes in the cells of salivary glands. Comparative genomics in *Drosophila* began when mapped morphological traits were used to establish the homologies of the chromosome arms of closely related species (Donald 1936; Sturtevant and Tan 1937; Muller 1940; Sturtevant and Novitski 1941). Muller (1940) codified this effort by assigning a letter to every chromosome arm or element common to all the species using *Drosophila melanogaster* as the model. According to this standard nomenclature, the A element corresponds to the X chromosome, B and C, respectively, to arms 2L and 2R, D and E to 3L and 3R, with F corresponding to chromosome 4 (Fig. 1).

While early studies showed that the genes are syntenic or at least conserved on the same chromosome arms among the species (Sturtevant and Novitski 1941), increasing numbers of physical and genetic markers on the polytene maps, revealed that the order of genes within the Muller elements is not conserved among species (Ranz *et al.* 2001). Moreover, a wealth of variability in gene arrangements on every chromosomal arm is found to be greater when comparing more distantly related species (Sperlich and Pfriem 1986; Bhutkar *et al.* 2008). This variability is manifest in a comparison of polytene chromosomes among closely related species through which it is possible to reconstruct the evolutionary history of the rearrangements (Dobzhansky 1944; Lemeunier and Ashburner 1976). Unfortunately, the banding pattern of the polytene chromosomes of more distantly related species is not comparable at least in part because of the accumulation of numerous rearrangements.

Drosophila melanogaster has been an exceedingly important model organism since the beginning of modern genetics and its

Received: May 25, 2022. **Accepted:** August 01, 2022

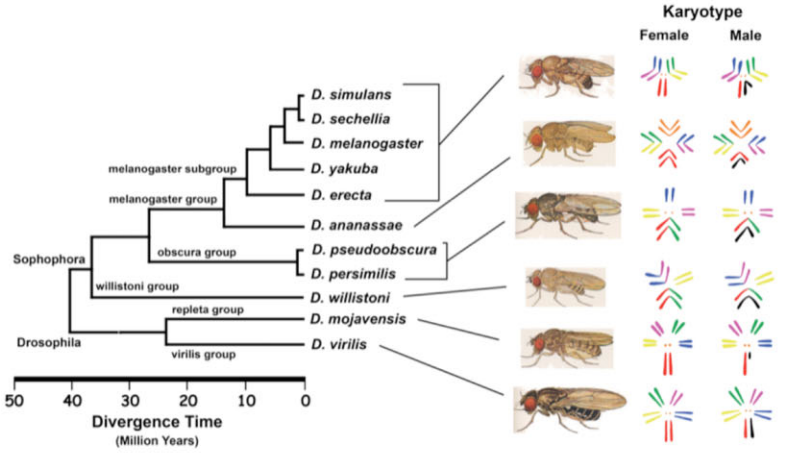

A	B	C	D	E	F
X	2L	2R	3L	3R	4
XLXR	3R	3L	2R	2L	4L4R
XL	4	3	XR	2	5
XL	2R	2L	XR	3	
X	3	5	4	2	6
X	4	5	3	2	6

Fig. 1. Syntenic relationships of chromosomal arms of the *Drosophila* species included in this study. To the left, a phylogenetic tree of the *Drosophila* species. To the middle, a representative fly image of a species of each group and the corresponding karyotype are depicted. To the right, the correspondence of the Muller elements and their standard chromosomal numbering showed in the table. The modified image from Crosby *et al.* (2007) and Flybase (http://flybase.org/maps/synteny, last accessed on 22 May 2022).

genome was one of the first to be sequenced (Adams *et al.* 2000). Subsequently, an additional 11 *Drosophila* species (*ananassae*, *erecta*, *mojavensis*, *persimilis*, *pseudoobscura*, *sechellia*, *simulans*, *virilis*, *willistoni*, *yakuba*, and *grimshawi*) were sequenced (Clark *et al.* 2007). More recently another 5 have been added (*biarmipes*, *bipectinata*, *eugracilis*, *mauritiana*, and *triauraria*; Miller *et al.* 2018). The number of sequenced genomes in the genus has continued to grow and of this writing 23 species from the Drosophila montium group have been added to the expanding data set (Bronski *et al.* 2020). This wealth of information offers an excellent opportunity to establish the global pattern of genomic evolution, at both genetic and chromosomal level. The analysis of the data derived from genomic sequencing has shed light on gene evolution in terms of length of introns, selective constriction on coding or noncoding sequences and other processes. The wide range of conservation of gene content inside the Muller elements is useful for scaffold assignment to specific chromosomal arms, but as noted above, gene order is poorly conserved due to the accumulation of multiple inversions and transpositions causing a reshuffling of gene order (Segarra and Aguadè 1992; Ranz *et al.* 2001). The cytogenetic maps of other *Drosophila* species represent a useful means to order genomic scaffolds mapped through a web-based format such as JBrowse on Flybase (http://flybase.org/, last accessed on 22 May 2022). The combined approaches of comparative analysis of syntenic blocks and direct physical mapping on polytene chromosomes has provided an elucidation of the orientation of genomic sequences and notably differences between heterochromatic and euchromatic regions (Schaeffer *et al.* 2008). One result from these analyses is evidence of striking differences in genome size apparently associated with the size and extent of heterochromatic sequences, which is reflected at least partially in DNA which is not assigned to specific scaffolds of centromeric regions in genomic assemblies (Schaeffer *et al.* 2008). These differences in genome size are particularly evident in species belonging to the subgenus *Drosophila* (Bosco *et al.* 2007; Schaeffer *et al.* 2008).

As noted, heterochromatin cannot be studied using the maps of polytene chromosomes because it is underreplicated, included in the chromocenter and therefore does not produce the banding patterns seen in the euchromatic arms. Nevertheless, for *D. melanogaster*, a cytological map of the heterochromatin has been produced using mitotic chromosomes from larval neuroblasts. This map subdivides the 4 *D. melanogaster* chromosomes into 61 discrete regions (h1–h61) depending on the differential staining of DNA following specific cytological treatments (Pimpinelli *et al.* 1975; Gatti and Pimpinelli 1992; Fig. 2).

Recently, *D. melanogaster* heterochromatin has been more extensively sequenced and assembled by whole-genome shotgun sequencing (Hoskins *et al.* 2002, 2007; Smith *et al.* 2007). Similar to euchromatin, several scaffolds have been assigned to the heterochromatic portions of the genome (Schaeffer *et al.* 2008). However, the gene content of these regions shows a remarkable variability among species. For example, some *D. melanogaster* heterochromatic genes appear distributed in the euchromatic portions of the genome in other species (Schulze *et al.* 2006; Schaeffer *et al.* 2008; Cotsworth *et al.* 2022).

With this new genomic sequence data, we thought that detailed cytological maps of the heterochromatin from several *Drosophila* species would be an important resource as an aid in the analysis of the multiple heterochromatic rearrangements which have occurred during evolution and to correlate the history of genome rearrangements with the origin of new species. This also provides a better understanding of the cause of conservation and stability of the heterochromatic vs eukaryotic portions of the genomes.

In this work, we elaborated cytological maps of mitotic heterochromatin in 10 sequenced *Drosophila* species. These maps highlight 2 apparently different paths for the evolution of the heterochromatin in the subgenera Sophophora and Drosophila, one path leads toward a progressive complexity of heterochromatin (Sophophora) and the other toward a progressive simplification (Drosophila).

These maps will also be useful for understanding how the heterochromatin was involved in and associated with chromosome arm reshuffling during evolution.

Materials and methods

The sequenced species used here were obtained from NDSSC, National Drosophila Species Stock Center (https://blogs.cornell.edu/drosophila/, last accessed on 22 May, 2022). Flies were maintained at 24°C on a standard medium containing cornmeal, yeast, sucrose, agar, and propionic acid as a mold inhibitor (except for *D. persimilis* and *mojavensis*). The diet for *D. persimilis* and *mojavensis* was banana

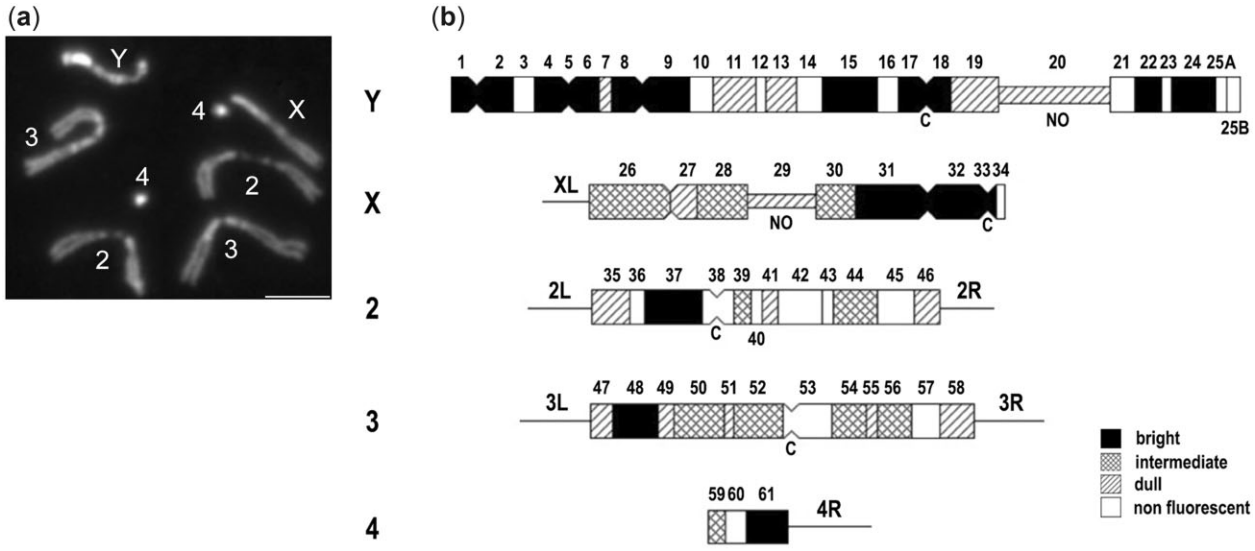

Fig. 2. Heterochromatin in *D. melanogaster*. a) A classical metaphase of larval neuroblasts; b) Diagrammatic representation of *D. melanogaster* heterochromatin map. The diagrams represent prometaphase neuroblast chromosomes stained with DAPI. As reported in the figure, filled areas indicate bright fluorescence, cross-hatched areas moderate fluorescence, hatched areas dull fluorescence, and open areas no fluorescence. The modified image from Flybase (http://fb2017_05.flybase.org/reports/FBsp00000001.html, last accessed on 22 May 2022). Scale bar indicates 5μm.

medium with the addition of *Opuntia* powder (recipes from Cornell College of Agriculture and Life Science, National Drosophila Species Stock Center, https://www.drosophilaspecies.com/recipes/banana-opuntia/).

Chromosome preparation

Mitotic chromosome preparations for DAPI staining and chromosomal in situ hybridizations (FISH) using fluorescently labeled BAC probes (FISH) were obtained as described in Fanti and Pimpinelli (2004) and Pimpinelli *et al.* (2000, 2010a, 2010b). Brains were dissected from third instar larvae in physiological solution (NaCl 0.7%) and transferred to hypotonic solution (sodium citrate 0.5%) for 8 min. After keeping the brains in fixing solution (methanol/acetic acid/water in ratio 5.5:5.5:1) for 30 s, they were transferred on siliconized coverslip in 45% acetic acid and squashed. Slides were frozen in liquid nitrogen and transferred in ethanol for 10 min. Preparations were counterstained with 0.1 μg/ml of 4′,6-diamidino-2-phenylindole (DAPI), dissolved in 2X Saline-sodium citrate (SSC) for 10 min, and mounted in Vectashield (Vector Laboratories).

To construct the heterochromatin maps of the sequenced *Drosophila* species, as was done for *D. melanogaster* (Gatti and Pimpinelli 1992), we performed similar cytological analysis and banding procedures through a qualitative assessment of fluorescence intensity. . This qualitative approach was validated by quantitative analysis of the fluorescence intensity by using ImageJ software with 2 different methods. We randomly chose 3 different images of Y chromosomes, converted them from RGB to 8-bit grayscale and analyzed the fluorescence intensity by using both the "Plot Profile" application (Supplementary Fig. 1) and the corrected total fluorescence method described in Casale *et al.* (2022). The scaled length of the bands was validated by using Photoshop software (ruler tool) as in Piacentini *et al.* (2019).

In addition, to cytologically identifying the corresponding mitotic chromosome arms (Muller elements) among all the species, we employed fluorescent in situ hybridization (FISH) using specific heterologous cross-hybridizing DNA probes corresponding to syntenic euchromatic genes of *D. melanogaster* and sequences of specific *D. pseudoobscura* genes. The Muller elements were identified by using appropriated BAC clones selected from the "BACPAC Resource Center" (https://bacpacresources.org/, last accessed on 22 May, 2022). The selected clones, their associated marker genes and map positions in *D. melanogaster* are shown in Table 1.

In addition, to the *D. melanogaster* BACs, we used clones derived from *D. pseudoobscura* to identify the chromosome arms of *D. persimilis* and *pseudoobscura*. These are listed in Table 2.

Preparation of BAC DNA

Extraction of BAC DNA was as follows: a bacterial culture was seeded in 10 ml of LB medium with antibiotic (20 mg/ml chloramphenicol). Two milliliters of the overnight culture were centrifuged for 50 s at 13,000 rpm. The bacterial pellet resuspended in 100 μl of 50 mM TRIS-HCl, pH 8.5, 10 mM EDTA buffer. Then 200 μl fresh 0.2 M NaOH, 1% SDS solution was added. The tubes were inverted to mix and immediately 150 ml of 7.5 M ammonium acetate solution was added. The tubes were again inverted to mix. After centrifugation at 13,000 rpm for 15 min, the supernatant was transferred to a 1.5 ml microcentrifuge tube with 300 μl of isopropanol. After mixing by inversion, the preparation was centrifuged at 13,000 rpm for 10 min. The pellet and the walls of the tube were washed with 300 μl of 70% ethanol; the preparation was then centrifuged at 13,000 rpm for 5 min, and the pellet air-dried. The pellet was resuspended in 50 μl of 10 mM TRIS-HCl, pH 8, 1 mM EDTA buffer containing 50 μg/ml RNase A. This was followed by incubation at 65°C for 10 min. The DNA was stored at 4°C for short-term use.

Fluorescent in situ hybridizations

The BAC DNA probes were differentially labeled using a rhodamine or biotin coupled dUTP by nick-translation and in situ hybridization on mitotic chromosomes from larval brains was executed as reported (Pimpinelli *et al.* 2010b), in particular after hybridization at 37°C overnight, and 3 washes in 2X SSC at 50°C, signal was detected with anti digoxigenin–rhodamine (Roche Diagnostics) at a 1:100 dilution, or with antibiotin-FITC (Vector Laboratories) diluted 1:300 for 1 h at 37°C. DNA was

Table 1. Selected clones, their associoated marker genes and map positions in *D. melanogaster*.

Muller Element	Dmel Arm	Gene Name	Gene Symbol	FB ID	Dmel CG	Recombination Map Position	Cytological Map position	Sequence Location	BAC for Probe
B	2L	*roundabout 2*	*robo*	FBgn0002543	CG5481	2L-3	22A1-22A1	2L : 1,380,086.. 1,420,453 [−]	BACR16D07
B	2L	*Sirtuin 1*	*Sirt1*	FBgn0024291	CG5216	2L-47	34A7-34A7	2L : 13,165,564.. 13,169,551 [+]	BACR27F17
C	2R	*Cyclin-dependent kinase 5*	*CdK5*	FBgn0013762	CG8203	2R-74	52A13-52A13	2R : 15,569,528..15, 571,417 [−]	BACR48C01
D	3L	CG32264	CG32264	FBgn0052264	CG32264	3L-8	63E8-63F1	3L : 3,714,826.. 3,806,459 [−]	BACR10I10
E	3R	*pasilla*	*ps*	FBgn0261552	CG42670	3R-48	85D17-85D17	3R : 9,417,940. 9,455,500 [+]	BACR19J06

Table 2. Selected clones, their associoated marker genes and map positions in *D. persimilis* and *D. pseudoobscura*.

Muller Element	Dpse Arm	Dmel Gene Name	Dmel Gene Symbol	FB Dpse ID	FB Dpse GA	NCBI Gene ID	NCBI Symbol	NCBI Sequence Location	BAC for Probe
A	XL	*Proteasome regulator gamma*	*Reg*	FBgn0074052	GA14020	32274	No data	no data	CH1226-69A15
B	4	*Sirtuin 1*	*Sirt1*	FBgn0078743	GA18743	4816584	LOC4816584	NC_046681.1: 8659800-8663551 [+]	CH1226-68A2
C	3	*Cyclin-dependent kinase 5*	*CdK5*	FBgn0080884	GA20894	4804076	LOC4804076	NC_046680.1: 9833015-9834467 [−]	CH1226-66P19
E	2	*Mucin related 89F*	*MUR89F*	FBgn0038492	GA27121	42080	No data	No data	CH1226-60J8

counterstained with DAPI before image capture, using a cooled CCD camera mounted on a microscope.

To localize the Nucleolar Organizer (NO), we performed fluorescent in situ hybridization on mitotic chromosomes from larval brains as described in Pimpinelli et al. (2010b). A probe for the 18S rDNA was prepared by amplifying a 1,514-bp fragment from D. melanogaster genomic DNA using the primers 18S-F 5′-AGCGATCGCAA GATCGTTAT-3′ and 18S-R 5′-AATCCCAAGCATGAAAGTGG-3′.

Immunofluorescence assays

To cytologically identify the centromeres, we performed immunofluorescence experiments using anti-CID (for *D. simulans*, *D. sechellia*, *D. erecta*, *D. pseudoobscura*, *D. virilis*, and *D. mojavensis*), anti-BUB (for *D. yakuba*, *D. persimilis*, and *D. willistoni*), or anti Cenp-C (for *D. ananassae*) antibodies as indicated in the figures.

Mitotic chromosomes from brains for anti-CID immunostaining were prepared according to Pimpinelli *et al.* (2011). Briefly, brains were dissected from third instar larvae in physiological solution and transferred to hypotonic solution for 8 min. Brains were then transferred to a drop of chromosome isolation buffer (6 mM $MgCl_2$, 1% citric acid, and 1%Triton-X100), placed on a siliconized coverslip, dissociated using syringe needles, and squashed in the same solution. Slides were frozen in liquid nitrogen, transferred to cold methanol at −20°C for 5 min and then in acetone at −20°C 1 min for anti-CID immunostaining, or in 4% formaldehyde 10 min for anti-Cenp-C immunostaining, washed in 1X PBS for 5 min, permeabilized in 1X PBS and 1% Triton-X100 for 10 min, blocked in 1X PBS, and 5% nonfat dried milk for 30 min, and processed for immunofluorescence.

For Bub immunofluorescence brains were incubated in fix solution 1 for 1 min (2% formaldehyde, 2% Triton-X 100, 10 mM sodium phosphate pH 7, 0.1 mM NaCl) for 1 min, in fix solution 2 (45% acetic acid, 2% formaldehyde, 2% Triton-X 100, 10 mM sodium phosphate pH 7, 0.1 mM NaCl) for 2 min, and squashed with a siliconized coverslip. Slides were immersed in liquid nitrogen, washed in TBST (10 mM Tris HCl pH 8, 150 mM NaCl, 0.05% Tween-20), incubated in TBSTB (TBST added with 10% FBS) for 1 h.

Incubation with the primary antibody was carried at room temperature for 1 h and at 4°C overnight. The primary antibodies were diluted in 1X PBS and 1% BSA as follows: chicken anti-CID (1:100, Blower and Karpen 2001), guinea pig anti-Cenp-C (1:300, kindly provided by Mellone B.). Rabbit anti-Bub1 antibody Rb666 (kindly provided by Sunkel C.E.) was diluted 1: 1,000 in TBSTB. Primary antibodies were detected with Alexa Fluor 555 goat anti-chicken (1:300), Alexa Fluor 488 goat anti-rabbit (1:300), and Alexa Fluor 488 goat anti-guinea pig (1:300; from Thermo Fisher Scientific). The incubation with secondary antibodies was carried out at room temperature for 2 h. Washes during immunostaining were 3 × 5 min in 1X PBS or TBST for Bub1. After immunostaining preparations were counterstained with 0.1 μg/ml of DAPI, dissolved in 2X SSC for 10 min and mounted in Vectashield (Vector Laboratories). Chromosomes images were captured using a computer-controlled microscope equipped with a cooled CoolSnap CCD camera. The fluorescent signals, recorded separately as grayscale digital images, were pseudocolored and merged using AdobePhotoshop.

Results and discussion

To determine cytogenetic maps of the heterochromatin of representative sequenced *Drosophila* species, mitotic chromosomes from larval neuroblasts were stained by DAPI. The correspondence of the different chromosome arms (Muller elements) in the different species was established by FISH using as probes

syntenic gene sequences of *D. melanogaster*, except for *D. persimilis* and *D. pseudoobscura* for which sequences of specific *D. pseudoobscura* genes have been used. The centromeres were localized by using antibodies directed against CID or BUB proteins depending on the species (Sharp-Baker and Chen 2001; Vigneron *et al.* 2004). The sequenced species investigated here were: *D. melanogaster*, *D. simulans*, *D. sechellia*, *D. erecta*, *D. yakuba*, *D. ananassae*, *D. pseudoobscura*, *D. persimilis* and *D. willistoni* from the Subgenus Sophophora; *D. virilis* and *D. mojavensis* from the Subgenus Drosophila.

Some of the investigated species are phylogenetically distant, while others are more closely related. The genome size, the number of genes, and the features of the transposon types are very similar among the 12 genomes (Clark *et al.* 2007). A comparison of the euchromatic gene order and arrangements reveal that there have been numerous rearrangements within the euchromatic chromosome arms as well as fusions of arms which are separate in some species. About 95% of the genes are syntenic and inversions appear to be the main mechanism producing changes within chromosome arms among the genomes and arm-to-arm fusions which alter linkage relationships.

Subgenus Sophophora

Maps of the species of melanogaster *group*

The sequenced species most closely related to *D. melanogaster* are *D. simulans*, *D. sechellia*, *D. erecta* and *D. yakuba*. All of them are morphologically very similar and their karyotype consists of an acrocentric X chromosome, an entirely heterochromatic Y chromosome, 2 large metacentric autosomes and a dot fourth chromosome.

Drosophila melanogaster

Drosophila melanogaster heterochromatin is subdivided in 61 discrete bands with different fluorescence intensities, as described in Gatti and Pimpinelli (1992). In particular, the Y chromosome contains 25 regions (h1–h25), the X chromosome 9 regions (h26–h34), each autosome 12 regions (h35–h46 and h47–h57) and the fourth chromosome 4 regions (h58–h61). Two regions with different condensation level, the NO, are evident on sex chromosomes. We used this cytological map as the reference for the maps developed for the other species.

Drosophila simulans

Similar to *D. melanogaster*, DAPI staining reveals that in *D. simulans*, the entire Y chromosome, about 30% of the X chromosome, the pericentromeric region of the autosomes and most of chromosome 4 are cytologically heterochromatic (Fig. 3, a–c). Based on fluorescence intensities, the heterochromatic domains can be subdivided in 45 different regions (Fig. 3d). The Y chromosome contains fewer bands (h1–h17) and only 2 constrictions as compared to *D. melanogaster*, in which the Y chromosome contains 25 regions and 4 constrictions. The centromere is localized in the h12 region and unlike *D. melanogaster*, the Y short arm does not show a constriction suggesting the absence of an NO. This is confirmed by the absence of hybridization signals with an 18S ribosomal probe (Fig. 3c). Regarding the fluorescence patterns of the autosomes: the heterochromatin of the left arm of chromosome 2 (h24–h26) appears like that of *D. melanogaster*, whereas the right arm (h28–h32) shows fewer bands, specifically lacking 2 large dark regions (h42 and h45) that are present in *D. melanogaster*. Comparing chromosome 3 (h33–h42), 2 main differences are clear between *D. simulans* and *D. melanogaster*. The left arm of *D. simulans* clearly lacks 2 regions (h51 and h52) that are present in *D. melanogaster* and the fluorescence of the heterochromatic bands is generally more intense as compared to *D. melanogaster*. The banding pattern of chromosome 4 (h43–h45) appears cytologically conserved between the 2 species.

Drosophila sechellia

As shown in Fig. 4, the heterochromatin can be subdivided in 38 regions with a cytological pattern showing differences with respect to the patterns of both *D. melanogaster* and *D. simulans*. The banding pattern of the short arm of the Y chromosome appears like those of the 2 other species except for the fluorescent

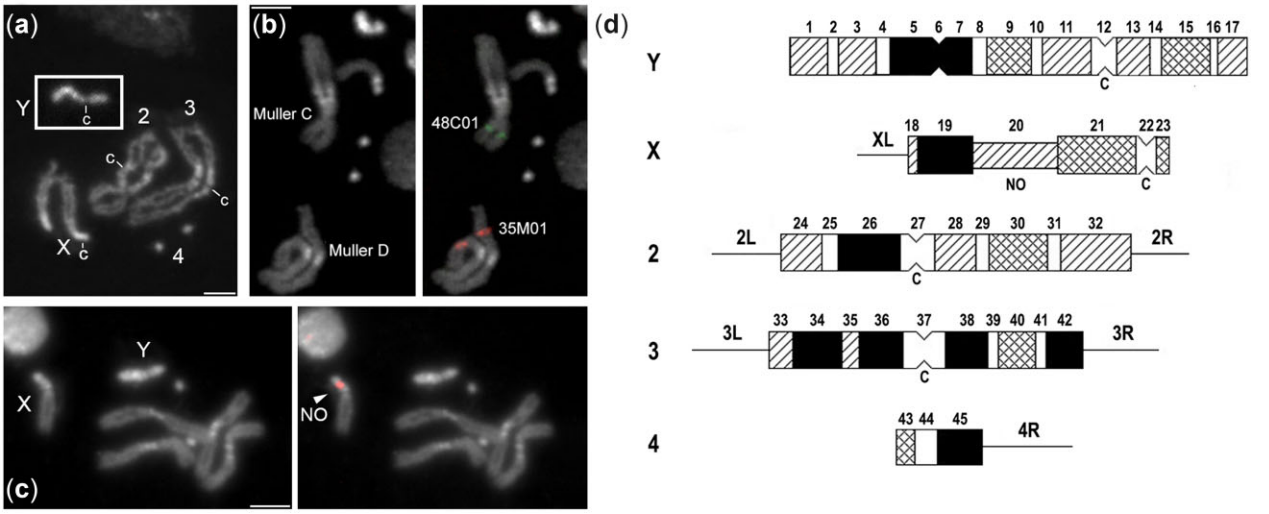

Fig. 3. Mitotic chromosomes of larval neuroblasts stained with DAPI from *D. simulans*. a) A prometaphase as an example. The Y chromosome in the white box comes from another prometaphase; b) Dapi staining (left panel) and localization of BACS 48C01 and 19J06 (right panel) on the same metaphase; c) Dapi staining (left panel) and localization of 18S rDNA probe to NO (right panel). The signal is localized in the X heterochromatin. The numbers indicate the autosomes; X, X chromosome and Y, Y chromosome; c indicates the centromere; d) Diagrammatic representation of *D. simulans* heterochromatin map. The diagrams represent prometaphase neuroblast chromosomes stained with DAPI. The filled areas indicate bright fluorescence, cross-hatched areas moderate fluorescence, hatched areas dull fluorescence, and open areas no fluorescence. Scale bar indicates 5μm.

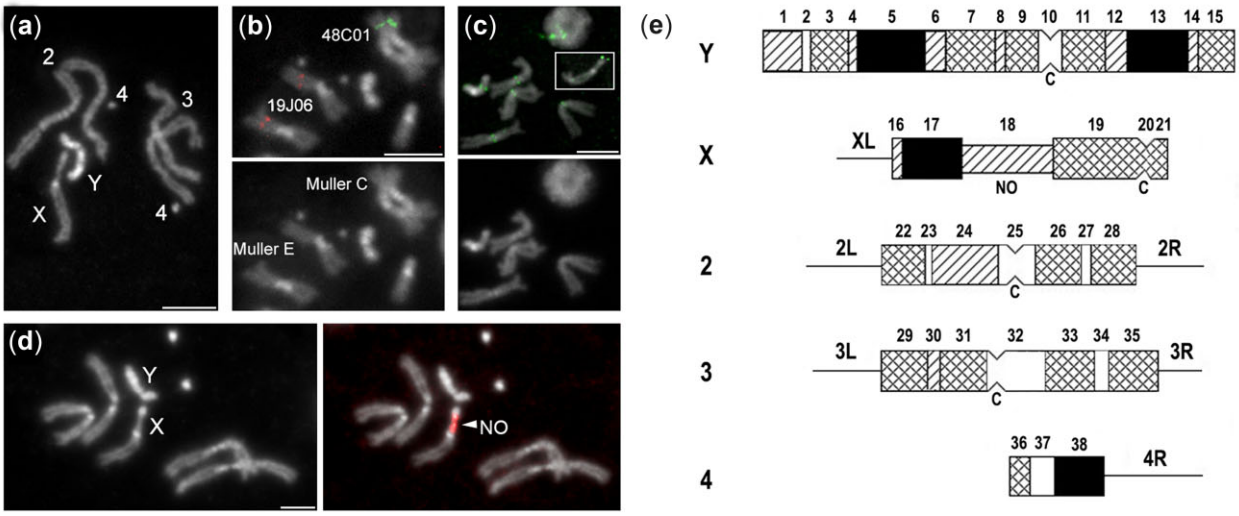

Fig. 4. Mitotic chromosomes of larval neuroblasts stained with DAPI from *D. sechellia*. a) A prometaphase as an example; b) Dapi staining (lower panel) and localization of BACS 48C01 and 19J06 on the indicated Muller elements (upper panel); c) Dapi staining (lower panel) and localization of CID on the centromeres (upper panel). The X chromosome in the white box comes from another prometaphase; d) Localization of 18S probe to NO. The signal is localized in the X heterochromatin. The numbers indicate the autosomes; X, X chromosome and Y, Y chromosome; e) Diagrammatic representation of *D. sechellia* heterochromatin map. The diagrams represent prometaphase neuroblast chromosomes stained with DAPI. Filled areas indicate bright fluorescence, cross-hatched areas moderate fluorescence, hatched areas dull fluorescence, and open areas no fluorescence. Scale bar indicates 5μm.

intensity of some of the blocks that appear greater while others dimmer. In addition, similar to *D. simulans* there is no NO in Y short arm (Fig. 2d). The fluorescent pattern of the Y long arm appears like that of *D. simulans* but different from that of *D. melanogaster* in both the number of bands and their dimmer fluorescence intensity. The heterochromatic pattern of the X chromosome is like the X chromosome of *D simulans* but is completely different from that of *D. melanogaster*. Regarding the autosomal heterochromatin: The cytological patterns are like the heterochromatin of *D. simulans* but lack the distal regions of both arms of chromosome 3 and the right arm of chromosome 2. In addition, fluorescence appears less bright as compared to *D. simulans* and like that of *D. melanogaster*.

Drosophila yakuba

The heterochromatin is subdivided in 33 regions and the banding pattern is different from that of *D. melanogaster* (Fig. 5). The Y chromosome is acrocentric, unique among these species, but this is probably not due to the absence of the entire short arm. The proximal regions (h5–h11) appear like the long arm regions of *D. simulans* and the distal regions (h1–h3) appear like the short arm regions (h13–h17) of the same species suggesting a pericentric inversion. Thus, the centromere appears to be repositioned, through the inversion. The X heterochromatin is cytologically conserved with *melanogaster* except for loss of h27–h28 and h30 regions. It is possible that a small proximal inversion has occurred moving part of the 16 bright regions into telomeric position (region 18). Regarding the autosomes: The heterochromatin of chromosome 2 appears to be inverted relative to other members of the melanogaster subgroup. The cytological and molecular characterization of this species (Schaeffer *et al.* 2008) demonstrated the presence of a pericentric inversion of this chromosome relative to its close relatives and this pattern in the heterochromatic banding pattern is consistent with that observation. This inversion is particularly evident when comparing *D. yakuba* with *D. simulans* heterochromatin, in which *D. simulans* h26, h28, h29, and h30 appear to be cytologically similar to *D. yakuba* h23, h19, h20, and h21, respectively. These last 3 regions also appear very similar to the 2L regions of *D. sechellia* (h22–h24). The heterochromatin of chromosome 3 shows fewer regions with respect to all the other species of the same group but very similar to the pericentromeric regions of *D. simulans* (h35–h40).

Drosophila erecta

As shown in Fig. 6, the heterochromatin of this species is subdivided in 23 regions. The heterochromatic banding pattern is more rearranged than when comparing *D. yakuba* to *D. melanogaster*. Thus, a comparison is possible only between the sister species *D. erecta* and *D. yakuba*. The Y chromosome lacks the *D. yakuba* h1 region and h5–h10 regions (h4 in *D. erecta*) are homogeneous in fluorescence intensity. Furthermore, the NO region is located close to the centromere at the end of the chromosome. The X chromosome contains 4 short bands with the NO in the h10 region close to h11 containing the centromere and the h8 and h9 regions homologous to h16 and h17, respectively, of *D. sechellia* and h18 and h19 regions of *D. simulans*. The second chromosome lacks the h21 region of *D. yakuba* but the other regions appear very similar in the 2 species. The third chromosome shows the h21 and h22 regions like the h29 and h30 regions of *D. yakuba* while the h18 and h20 regions apparently show no homology with the h26 and h27 regions of *D. yakuba*. Centromeric region h19 of *D. erecta* is located between h18 and h20, while the h26 and h27 regions of *D. yakuba* are at the same side of centromeric region h28. Furthermore, these regions show a different fluorescence intensity pattern.

Drosophila ananassae

This species is part of the melanogaster group, but not of *melanogaster* subgroup. The heterochromatin is subdivided in 48 regions thus this species has the highest number of heterochromatic regions after *D. melanogaster*. As shown in Fig. 7, D. *ananassae* has a karyotype characterized by a large metacentric X chromosome. The left arm (h13–h15 regions) is like the h26–h28 regions of *D. melanogaster* except that the h15 region of *D. ananassae* has a brighter fluorescence intensity than the h28 region of *D.*

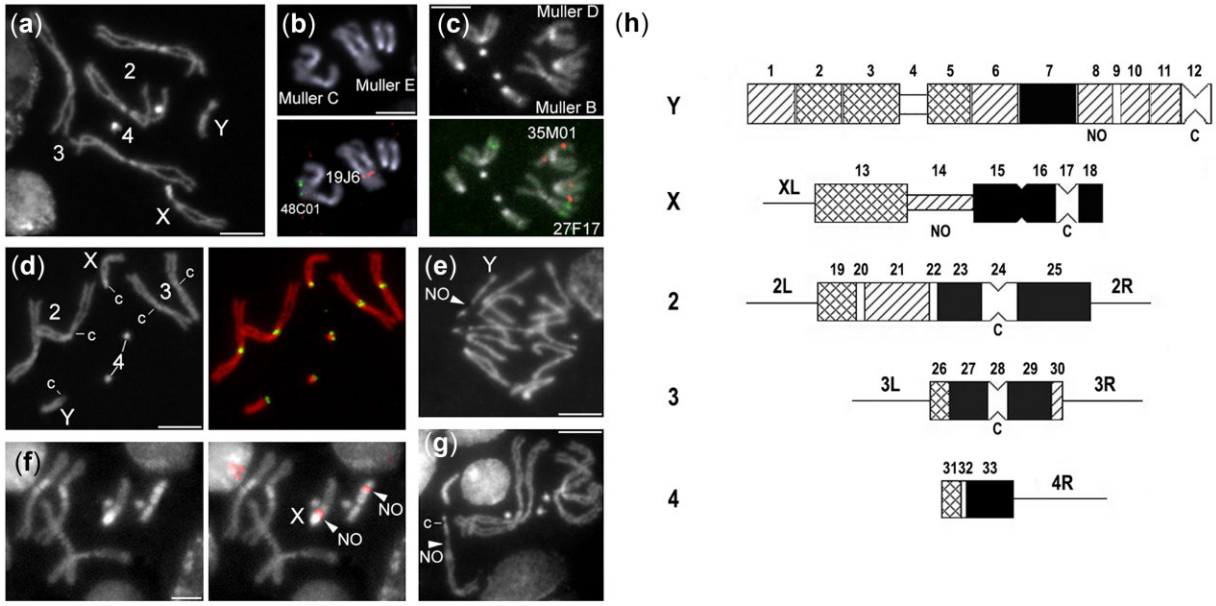

Fig. 5. Mitotic chromosomes of larval neuroblasts stained with DAPI from *D. yakuba*. a) A prometaphase as an example; b, c) Dapi staining (upper panels) and localization of BACS on the Muller C (48C01) and E (19J06) elements (b), Muller B (27F17) and D (35M01) elements (c) from larval brain neuroblast (lower panels). The green and red signals indicate 2 different probes on the same metaphase; d) Localization of BUB to the centromeres; e) Anaphase in which is shown the NO constriction of the Y chromosome; f) Localization of 18S probe to NO. The signals are localized on the X and Y heterochromatin; g) metaphase in which is shown the NO constriction of the X chromosome; the numbers indicate the autosomes; X, *X* chromosome and Y, *Y* chromosome, NO indicates NO and c, centromere; h) Diagrammatic representation of *D. yakuba* heterochromatin map. The diagrams represent prometaphase neuroblast chromosomes stained with DAPI. As reported in the figure, filled areas indicate bright fluorescence, cross-hatched areas moderate fluorescence, hatched areas dull fluorescence, and open areas no fluorescence. Scale bar indicates 5μm.

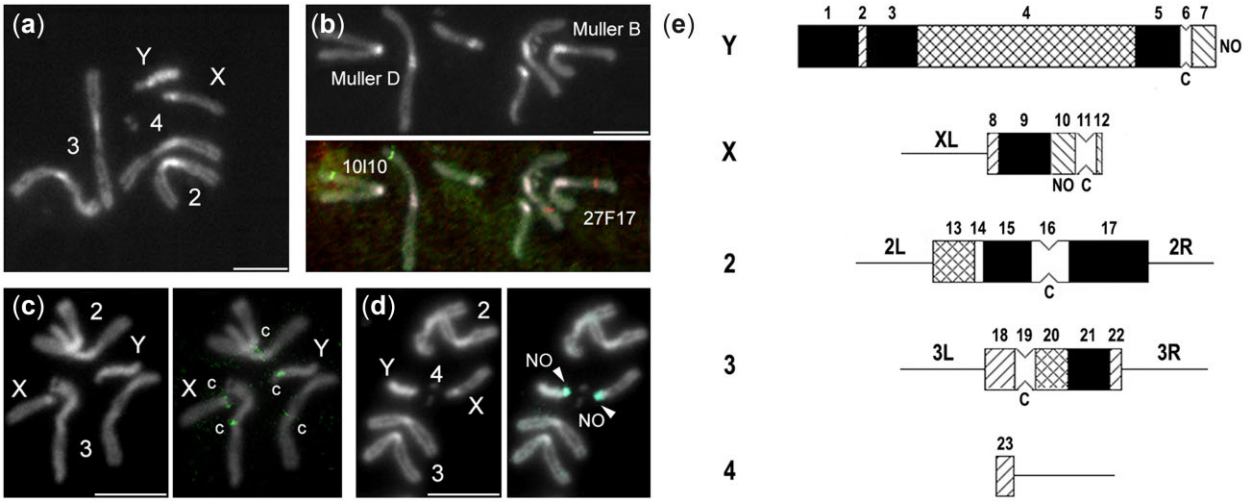

Fig. 6. Mitotic chromosomes of larval neuroblasts stained with DAPI from *D. erecta*. a) A prometaphase as an example; b) Dapi staining (upper panel) and localization of BACS (lower panel) on the Muller elements from larval brain neuroblast. The green (10l10) and red (27F17) signals indicate 2 different probes on the same metaphase; c) Localization of CID to the centromeres; d) Localization of 18S probe to NO. The signal is localized in the X heterochromatin. The numbers indicate the autosomes; X, *X* chromosome and Y, *Y* chromosome; e) Diagrammatic representation of *D. erecta* heterochromatin map. The diagrams represent prometaphase neuroblast chromosomes stained with DAPI. Filled areas indicate bright fluorescence, cross-hatched areas moderate fluorescence, hatched areas dull fluorescence, and open areas no fluorescence. Scale bar indicates 5μm.

melanogaster. An NO region does not map to the X chromosome (Fig. 7e).

The Y chromosome contains 3 bright fluorescent blocks on the long arm (h1, h3, and h5) like those of distal regions of *D. melanogaster*, as well as a proximal intermediate fluorescent region. On the short arm, there are 2 bright fluorescent blocks proximally, one intermediate fluorescent block and a distal NO. This part of the chromosome resembles the inverted short arm of the *D. sechellia* Y chromosome. The autosomes, including the fourth chromosome, are also large and metacentric. Arms 2L and 2R correspond, respectively, to E and D Muller elements while 3L and 3R correspond, respectively, to the C and B Muller elements. The autosomes appear to be very different from those of the other melanogaster group species. However, a resemblance of chromosome 2 of *D. ananassae* to chromosome 3 of *D. erecta* and *D. yakuba* can be envisioned if one postulates an inversion of the

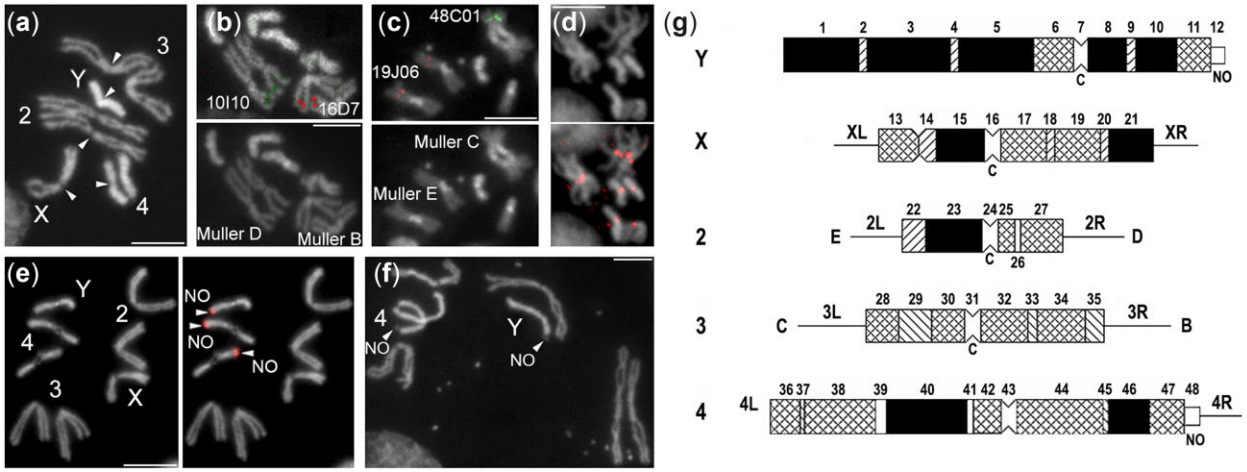

Fig. 7. Mitotic chromosomes of larval neuroblasts stained with DAPI from *D. ananassae*. a) A prometaphase as an example; b, c) Dapi staining (lower panels) and localization of BACS (upper panels) on Muller B (16D7) and D (10l10) elements (b), Muller C (48C01) and E (19J06) elements (c) from larval brain neuroblast. The green and red signals indicate 2 different probes on the same metaphase; d) Localization of CENP-C to the centromeres; e) Localization of 18S probe to NO. The signals are localized in the Y and 4 heterochromatin; f) metaphase in which are shown the NO constrictions (arrowheads) of the Y and 4 chromosomes. The numbers indicate the autosomes; X, X chromosome and Y, Y chromosome; g) Diagrammatic representation of *D. ananassae* heterochromatin map. The diagrams represent prometaphase neuroblast chromosomes stained with DAPI. As reported in the figure, filled areas indicate bright fluorescence, cross-hatched areas moderate fluorescence, hatched areas dull fluorescence, and open areas no fluorescence. Scale bar indicates 5μm.

arms. Furthermore, a resemblance can be observed comparing chromosome 3 of *D. ananassae* with chromosome 2 of *D. sechellia*. *Drosophila ananassae* is the only species among those analyzed that has a large heterochromatic metacentric chromosome 4, with 2 pairs of bright fluorescent blocks separated by the centromeric region. Despite a different fluorescence intensity this chromosome appears very similar to the Y chromosome also containing also an NO in the telomeric position of the right arm.

Maps of the species of obscura group

The species of *obscura* group are characterized by the presence of 4 acrocentric autosomes, one of them a dot and a metacentric X chromosome. The left arm of chromosome X (XL) corresponds to Muller element A, while the right arm corresponds to the D element. The autosomes 2, 3, 4, and 5 correspond to the E, C, B, and F elements, respectively (Crosby *et al.* 2007). The Y chromosome carries some genes belonging to the D element, suggesting it could be a degenerated autosome (Carvalho and Clark 2005).

Drosophila pseudoobscura

According to the hypothesis of a Y chromosome as a degenerated autosome, the heterochromatic pattern of the Y is completely different from the Y of the other species, except *D. persimilis*. As shown in Fig. 8, the Y chromosome shows 4 bright fluorescent blocks similar in size (h1, h5, h7, and h9) as well as other differently sized intermediate or dull fluorescent blocks. The h7–12 regions could be the result of a pericentric inversion with respect to h6–h10 regions of *D. ananassae*. This inversion is also evident in *D. persimilis* (h7–h12). The X heterochromatin has one bright fluorescent block (h18) and other regions showing intermediate fluorescence on left and right arms plus a dull region (h19) on the right arm that corresponds to an NO. The autosomes have a small and homogenous piece of heterochromatin. The h23 and h22 of chromosome 4 and 3, respectively, could have the same derivation as the h30 and h32 of the third chromosome of *D. ananassae*.

Drosophila persimilis

This is the sister species of *D. pseudoobscura* and this is evident also in the heterochromatic pattern of sexual chromosomes. As shown in Fig. 9, both the X and the Y chromosomes are fully comparable between the 2 species. The only exception is a double duplication of h12 and h13 regions (h14–h17) present in *D. persimilis* that is not seen in *D. pseudoobscura*. Furthermore, there is a difference in fluorescence intensity between the h14 region of the X chromosome of *D. pseudoobscura* and the h18 region of the same chromosome of *D. persimilis* which is brighter. Also, in this species, the autosomal heterochromatin consists of small and fluorescent homogeneous regions (h27, h28, h29, and h30 of the chromosomes 2, 3, 4, and 5 respectively).

Map of the species D. willistoni

The only member of the willistoni group examined here is *D. willistoni*. This species diverged basally to the obscura and melanogaster groups within the subgenus Sophophora. Therefore, we presume this species could be representative of a progenitor of the more derived species. As shown in Fig. 10, a–c, and diagrammatically reported in Fig. 10d, D. *willistoni* has a symmetric Y chromosome, with 2 pairs of bright fluorescent blocks lateral to the pericentromeric region (h1, h3 and h9, h11) which contains 2 intermediate fluorescent blocks (h5 and h7) separated by the centromere. An NO is located in the h8 region. The X chromosome has 2 bright fluorescent blocks (h13 and h19) separated by 2 intermediate fluorescent blocks (h15 and h17) between which the centromere is positioned. The chromosome 2 contains 5 bright fluorescent blocks (h20, h22, h24, h26, and h28) with the centromere submetacentrically positioned (h25). Chromosome 3 has less heterochromatin when compared to chromosome 2. It could also contain the heterochromatin of the chromosome of the Muller F element which is fused to this larger autosome (Schaeffer *et al.* 2008), although this is not detectable in the map. The third chromosome has a single bright fluorescent block (h32) and 3 dull blocks (h30, h34, and h36); the NO regions are visible on both Y- and X-chromosomes (h8 and h15; Fig. 8).

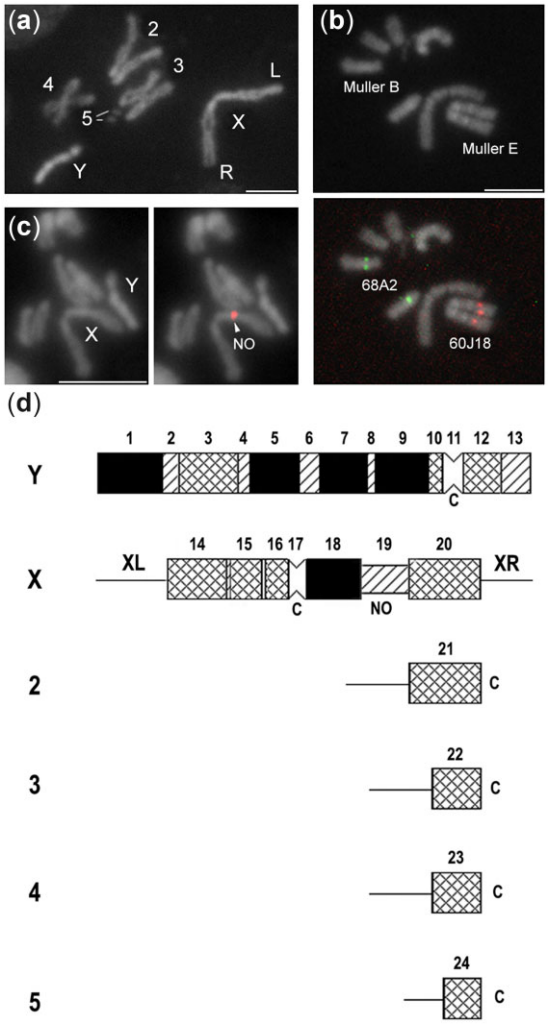

Fig. 8. Mitotic chromosomes of larval neuroblasts stained with DAPI from *D. pseudoobscura*. a) A prometaphase as an example; b) Dapi staining and localization of BACS on Muller B and E elements from larval brain neuroblast. The green (68A2) and red (60J18) signals indicate 2 different probes on the same metaphase; c) Localization of the 18S probe to NO. The signal is localized in the X heterochromatin. The numbers indicate the autosomes; X, X chromosome and Y, Y chromosome; d) Diagrammatic representation of *D. pseudoobscura* heterochromatin map. The diagrams represent prometaphase neuroblast chromosomes stained with DAPI. Filled areas indicate bright fluorescence, cross-hatched areas moderate fluorescence, hatched areas dull fluorescence, and open areas no fluorescence. Scale bar indicates 5μm.

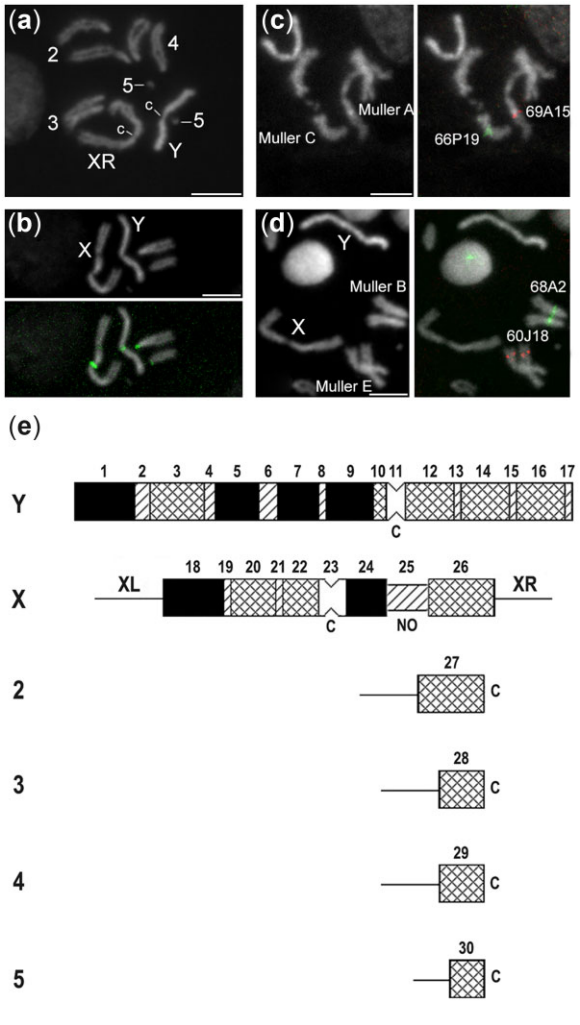

Fig. 9. Mitotic chromosomes of larval neuroblasts stained with DAPI from *D. persimilis*. a) A prometaphase as an example; b) Localization of BUB to the centromeres; c, d) Dapi staining (left panels) and localization of BACS (right panels) on the Muller A (69A15) and C (66P19) elements (C), Muller B (68A2) and E (60J18) elements (D) from larval brain neuroblast. The green and red signals indicate 2 different probes on the same metaphase; the numbers indicate the autosomes; X, X chromosome and Y, Y chromosome; e) Diagrammatic representation of *D. persimilis* heterochromatin map. The diagrams represent prometaphase neuroblast chromosomes stained with DAPI. Filled areas indicate bright fluorescence, cross-hatched areas moderate fluorescence, hatched areas dull fluorescence, and open areas no fluorescence. Scale bar indicates 5μm.

Subgenus Drosophila

This subgenus includes the sequenced species *D. mojavensis* from the repleta group and *D. virilis* from virilis group.

Map of the species D. mojavensis

As shown in Fig. 11, the karyotype consists of X and Y sex chromosomes, 4 acrocentric autosomes and a dot autosome. Muller elements are distributed in such a way that E element corresponds to chromosome 2, B corresponds to chromosome 3, D corresponds to chromosome 4, C corresponds to chromosome 5 and F corresponds to chromosome 6 (Crosby *et al.* 2007). The autosomes have a small and homogeneous portion of heterochromatin not represented in the map. Regarding the sex chromosomes, both Y and X have homogeneous heterochromatin with only 3 intermediate (h1, h3 for the Y and h4, h6 for the X) or dull (h2 for the Y and h5 for the X) fluorescent regions and both have an NO region. Regarding the autosomes, they show similar small blocks of dull fluorescent pericentromeric heterochromatin (not diagrammaticaly shown).

Map of the species D. virilis

Drosophila virilis karyotype appears very similar to *D. mojavensis* (Fig. 12), but Muller elements are enumerated differently: B element corresponds to chromosome 4, C corresponds to chromosome 5, D corresponds to chromosome 3, E corresponds to chromosome 2 and F corresponds to chromosome 6 (Crosby *et al.* 2007). In comparison with *D. mojavensis*, the metacentric Y chromosome of *D. virilis* contains 10 regions with variable fluorescence intensity, with 2 lateral distal intermediate fluorescent blocks (h2 and h10), and 8 dull (h1, h3, h5, h7, and h8) or not fluorescent (h4, h6, and h9) regions. The acrocentric X chromosome shows 3 small regions of heterochromatin: one bright fluorescent

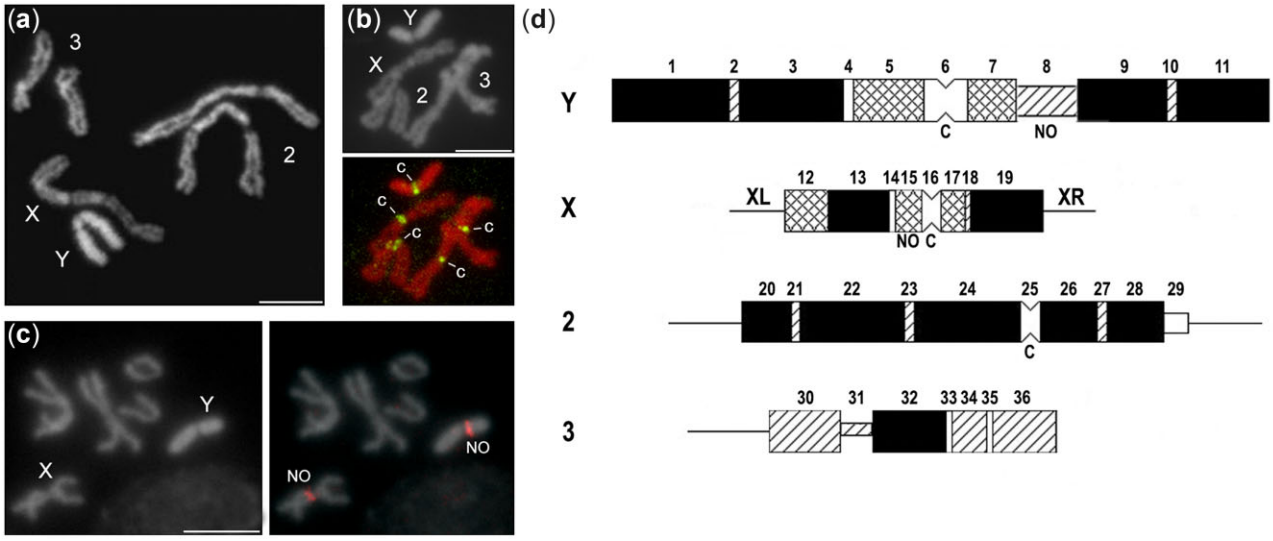

Fig. 10. Mitotic chromosomes of larval neuroblasts stained with DAPI from *D. willistoni*. a) A prometaphase as an example; b) Localization of BUB to the centromeres; c) Dapi staining and localization of 18S probe to NO. The signals are localized in the X and Y heterochromatin. The numbers indicate the autosomes; X, X chromosome and Y, Y chromosome; d) Diagrammatic representation of *D. willistoni* heterochromatin map. The diagrams represent prometaphase neuroblast chromosomes stained with DAPI. Filled areas indicate bright fluorescence, cross-hatched areas moderate fluorescence, hatched areas dull fluorescence, and open areas no fluorescence. Scale bar indicates 5μm.

region (h13) and another with intermediate fluorescence (h11) separated by one small dull fluorescent region containing the NO (h12). The *X* chromosomes of *D. virilis* and *D. mojavensis* appear very similar, except the distal region (h6 of *mojavensis* and h13 of *virilis*) which is brightly fluorescent in *D. virilis* and of intermediate fluorescence in *D. mojavensis*. The heterochromatin of the autosomes 2 and 4 appears similar with an intermediate (h14 and h20, respectively), a dull (h15 and h21, respectively) and a bright (h16 and h22, respectively) fluorescent regions. Likewise, the heterochromatin of the autosomes 3 and 5 appears similar with 3 regions (h17–h19 for the 3 and h23–h25 for the 5). The only difference is that the external regions of the third chromosome are dull and those of the fifth chromosome are intermediate fluorescent. The sixth chromosome contains only one small dull fluorescent region.

Conclusions

The genomic analysis of pericentric heterochromatin is essential to the study of chromosomes behavior and understanding karyotypic evolution. The presence of certain patterns is not the exclusive prerogative of the species in the genus *Drosophila*. These compartments of the genome appear to be conserved during the evolution of several eukaryotic genomes: some orthologs of heterochromatic genes of *D. melanogaster* (Corradini *et al.* 2007) have been found in yeast, mouse and human and have a euchromatic location (Kuhn *et al.* 1991; Horvath *et al.* 2000; Brun *et al.* 2003). The discovery of hundreds of heterochromatic genes in *Drosophila*, plants and mammals through sequencing projects offers unique opportunities to examine the different ways in which heterochromatin influences gene expression and the appearance of new species. The availability of detailed cytological maps of several *Drosophila* species enables the analysis of the multiple heterochromatic rearrangements that have taken place during evolution; it also provides the observation of their conservation or variation and an understanding of the stability of heterochromatin in the genomes of higher eukaryotes.

In this work, we have built the cytological map of the heterochromatin of 10 sequenced *Drosophila* species. The different quantity of heterochromatin and its variable fluorescence intensity likely reflects differences in both DNA base composition and protein composition and consequently different properties and functions. The emerging result is a constant increase of abundance and complexity of heterochromatin during evolution, at least for the Sophophora branch of the genus Drosophila. Only the *obscura* group seems to be an exception due to this pattern due to its poor autosomal heterochromatin (Fig. 13 and Supplementary Figs. 2–5).

Following the separation of Sophophora subgenus from *Drosophila* subgenus, about 40 million years ago, the branch containing the willistoni group was established early. Among the species under study, we speculate that *D. willistoni* represents a basal cytological pattern of heterochromatin and can be viewed as the progenitor of the Sophophora subgenus. This species has a metacentric X chromosome, in which the left arm, containing Muller A element, corresponds to the X in all species of the genus; the right arm containing the Muller D element, corresponds to the left arm of the Sophophora chromosome 3. This result is compatible with our heterochromatin map. The 17h–18h regions of the *D. willistoni* X chromosome overlaps with 25h–26h regions of the *D. ananassae* 2R chromosome, both containing the Muller D element.

Furthermore, *D. ananassae* is the only species among those sequenced that contains a big metacentric and fully heterochromatic chromosome 4. Based on the homology of the 4 heterochromatic blocks with the *willistoni* Y chromosome, there is the possibility that the fourth chromosome originated by the duplication of a Y chromosome present in the common ancestor of the Sophophora and Drosophila subgenera. Indeed, the *D. ananassae* chromosome 4 is very similar to the *D. willistoni* Y, although some blocks have a slight difference in fluorescent intensity. Furthermore, the *ananassae* Y chromosome is like the *D. willistoni* Y chromosome confirming that they are closer species to the common ancestor. Furthermore, chromosome 2 of *D. willistoni* is surprisingly like the Y chromosome of *D. ananassae*, also containing the NO in distal position of 2R and very different from the chromosome 2 of all the other species.

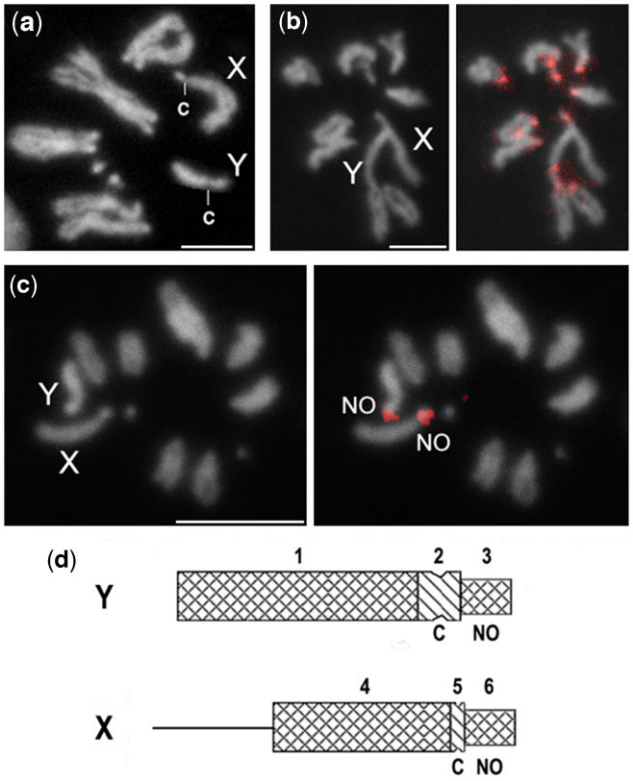

Fig. 11. Mitotic chromosomes of larval neuroblasts stained with DAPI from *D. mojavensis*. a) Mitotic chromosomes of larval neuroblasts stained with DAPI as an example; b) Dapi staining and localization of CID to the centromeres; c) Localization of 18S probe to NO. The signals are localized in the X and Y heterochromatin; d) Diagrammatic representation of *D. mojavensis* heterochromatin map. The diagrams represent prometaphase neuroblast chromosomes stained with DAPI. As reported in the figure, filled areas indicate bright fluorescence, cross-hatched areas moderate fluorescence, hatched areas dull fluorescence, and open areas no fluorescence. The pericentric heterochromatin of autosomes is not reported because, for all of them, corresponds to identical small blocks with homogeneous dull fluorescence Scale bar indicates 5μm.

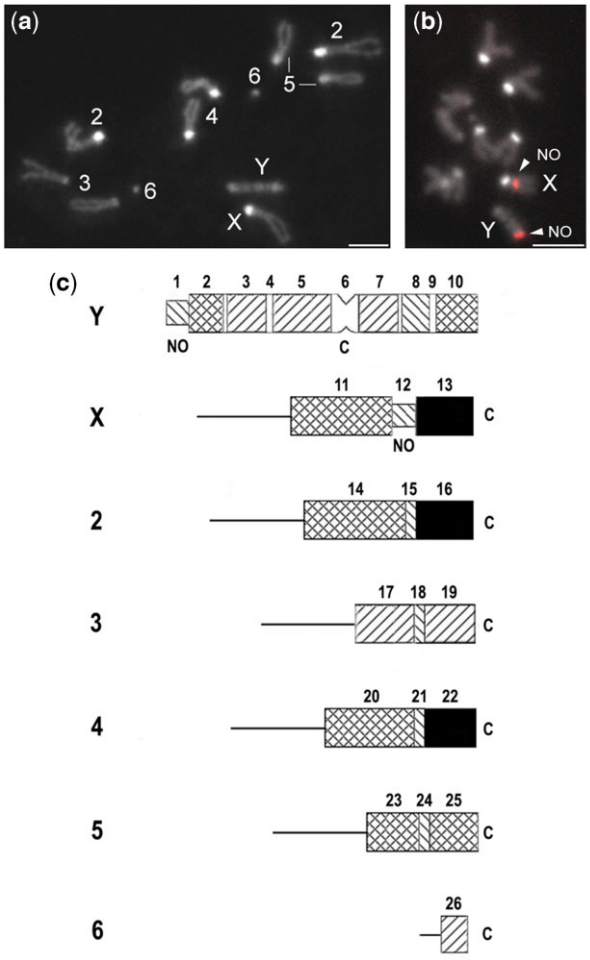

Fig. 12. Mitotic chromosomes of larval neuroblasts stained with DAPI from *D. virilis*. a) Mitotic chromosomes of larval neuroblasts stained with DAPI as an example; b) Localization of 18S probe to NO. The signals are localized in the X and Y heterochromatin; c) Diagrammatic representation of *D. virilis* heterochromatin map. The diagrams represent prometaphase neuroblast chromosomes stained with DAPI. Filled areas indicate bright fluorescence, cross-hatched areas moderate fluorescence, hatched areas dull fluorescence, and open areas no fluorescence. Scale bar indicates 5μm.

Five species among the 12 first sequenced belong to Sophophora subgenus: *D. melanogaster*, *D. simulans*, *D. sechellia*, *D. yakuba*, and *D. erecta*. Their karyotypes and the syntenic relations among the species show a closer relation of *D. sechellia* and *D. simulans*, with respect to *D. melanogaster* (Schaeffer *et al.* 2008). Our maps seem to confirm that the heterochromatic pattern of *D. simulans* is more homologous to the *D. sechellia* pattern. This major homology concerns both the sexual chromosomes and chromosome 2. With regards to chromosome 3, it appears that *D. simulans* is much richer in AT sequences with respect to both *D. melanogaster* and *D. sechellia*. Chromosome 4 has the same pattern in all 3 species.

Considering the entire heterochromatic pattern amongst Drosophila species, we notice a greater complexity in terms of variability in the content of AT-rich sequences during the evolution in the subgenus Sophophora and a simplification in the subgenus Drosophila starting from the common ancestor.

Since our maps show the relative abundance of base pairs based on the fluorescence intensity in the bands and do not show which genetic elements are contained in those bands, it is difficult to explain the significance of the different patterns by an evolutionary point of view. However, heterochromatin contains high levels of repetitive elements such as satellite DNA and transposable elements (TEs) belonging to different families. TEs are supposed to be an evolutionary force, since they are activated following various stressful conditions. The activation of transposons could increase genetical variability with strong evolutionary implications (see Piacentini *et al.* 2014 for a discussion). Among the species analyzed in the present study, *D. melanogaster* has the highest heterochromatin content and complexity and *D. mojavensis* the lowest. The first is the most widespread in the world and the second the least (Makino and Kawata 2012). *Drosophila sechellia* appears to be an exception, but this may be due to its recent divergence from *D. melanogaster*. This apparent correlation between TE abundance and geographical spread could explain the different heterochromatic complexity in the Sophophora and Drosophila subgenus.

With regards to the subgenus Drosophila, it will therefore be important to have a cytological map of *D. grimshawi* as well as other members of the group. Recently, additional species belonging to the melanogaster group of the subgenus Sophophora have been sequenced but it is also important to sequence genomes from additional species of the subgenus Drosophila to perform a more complete comparative analysis of all the mitotic heterochromatin maps thereby giving a broader understanding of karyotypic evolutionary mechanisms.

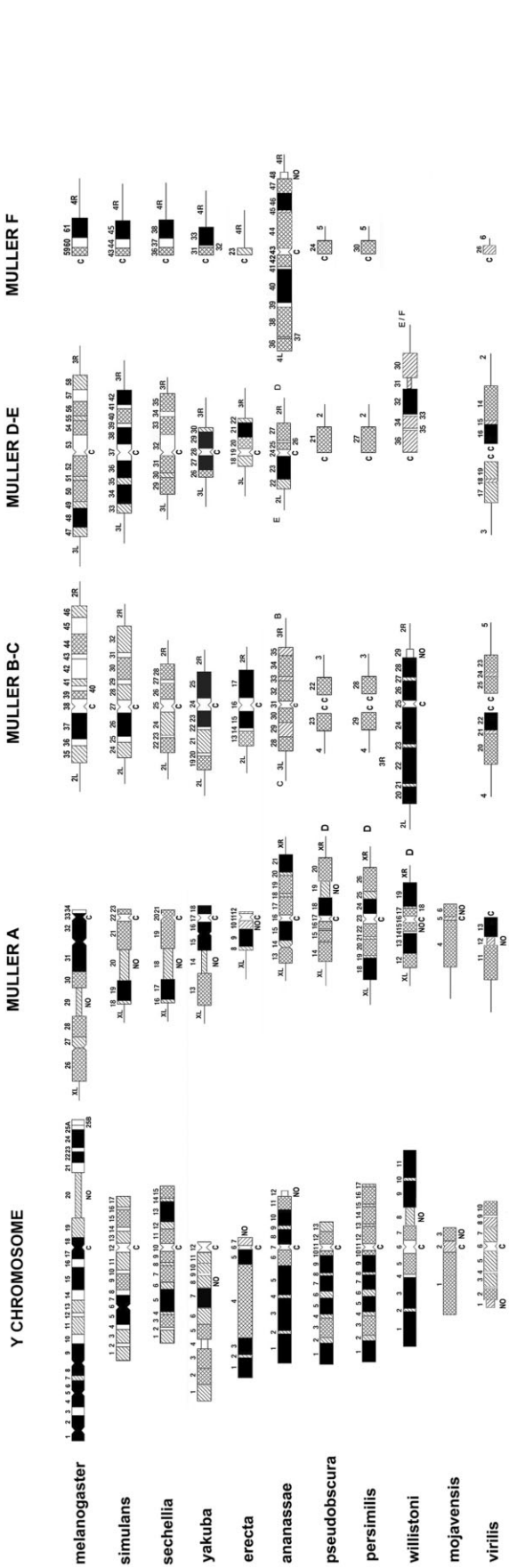

Fig. 13. Summary diagrammatic representation of the mitotic maps of heterochromatin with the karyotypic and syntenic relationships of the Muller elements for the indicated sequenced species of the genus *Drosophila*.

A possible path for the future

As noted, the polytene chromosomes are not usable for cytological mapping of constitutive heterochromatic regions since that genomic compartment is located inside the chromocenter and underreplicated. Rather, constitutive heterochromatin has been cytologically defined and well characterized in mitotic chromosomes from larval neuroblasts in *D. melanogaster*. It has been subdivided into specific subregions by virtue of blocks with different staining properties (Pimpinelli *et al.* 1975). Furthermore, a cytological map of "contigs," sets of genomic sequences with contiguous regions of DNA, has been elaborated within constitutive heterochromatin from both mitotic and polytene chromosomes using the Su(var)3-9, SuUR double mutants in *D. melanogaster* (Andreyeva *et al.* 2007). These genes code for structural heterochromatic proteins. Thus, animals carrying the double mutant alleles, due to suppression of underreplication, reveal novel banded regions in polytene chromosome preparations that are adjacent to the chromocenter and derived from the normally underreplicated heterochromatic blocks.

The in situ fluorescent hybridization technology by using of specific DNA probes performed on both double mutants polytenes and wild-type mitotic chromosomes has permitted a cytogenetic high-resolution map of heterochromatin (Andreyeva *et al.* 2007; Hoskins *et al.* 2007; Accardo and Dimitri 2010) and this type of analysis could and should be expanded to include additional species in the genus Drosophila.

Data availability

The authors affirm that all data necessary for confirming the conclusions of the article are present within the article, figures, and tables.

Supplemental material is available at GENETICS online.

Acknowledgments

We thank Gary Karpen, Barbara Mellone, and Claudio Sunkel for antibodies. Special thanks to Thomas Kaufman for the critical reading of the manuscript and helpful suggestions. This work was partly supported by the Epigenomics Flagship Project EpiGen, the Italian Ministry of Education and Research.

Funding

Financial support of this research was provided by the Epigenomics Flagship Project EpiGen, Italian Ministry of Education and Research, National Research Council and research project grants from Sapienza University of RomeRM118164280AAEF8

Conflicts of interest

None declared.

Literature cited

Accardo MC, Dimitri P. Fluorescence in situ hybridization with Bacterial Artificial Chromosomes (BACs) to mitotic heterochromatin of Drosophila. Methods Mol Biol. 2010;659:389–400.

Adams MD, Celniker SE, Holt RA, Evans CA, Gocayne JD, Amanatides PG, Scherer SE, Li PW, Hoskins RA, Galle RF, *et al.* The genome sequence of *Drosophila melanogaster*. Science. 2000;287(5461):2185–2195.

Andreyeva EN, Kolesnikova TD, Demakova OV, Mendez-Lago M, Pokholkova GV, Belyaeva ES, Rossi F, Dimitri P, Villasante A, Zhimulev IF. High-resolution analysis of *Drosophila* heterochromatin organization using *SuUR Su(var)3–9* double mutants. Proc Natl Acad Sci USA. 2007;104(31):12819–12824.

Auvinet J, Graca P, Dettai A, Amores A, Postlethwait JH, DetrichIII HW, Ozouf-Costaz C, Coriton O, Higuet D. Multiple independent chromosomal fusions accompanied the radiation of the Antarctic teleost genus Trematomus (Notothenioidei: Nototheniidae). BMC Ecol Evol. 2020;20:39. doi:10.1186/s12862-020–1600-3.

Bhutkar A, Schaeffer SW, Russo SM, Xu M, Smith TF, Gelbart WM. Chromosomal rearrangement inferred from comparisons of 12 *Drosophila* genomes. Genetics. 2008;179(3):1657–1680.

Blower MD, Karpen GH. The role of Drosophila CID in kinetochore formation, cell-cycle progression and heterochromatin interactions. Nat Cell Biol. 2001;3(8):730–739.

Bosco G, Campbell P, Leiva-Neto JT, Markow TA. Analysis of *Drosophila* species genome size and satellite DNA content reveals significant differences among strains as well as between species. Genetics. 2007;177(3):1277–1290.

Bronski MJ, Martinez CC, Weld HA, Eisen MM. Whole genome sequences of 23 species from the *Drosophila montium* species group (Diptera: Drosophilidae): a resource for testing evolutionary hypotheses. G3 (Bethesda). 2020;10(5):1443–1455.

Brun ME, Ruault M, Ventura M, Roizes G, De Sario A. Juxtacentromeric region of human chromosome 21: a boundary between centromeric heterochromatin and euchromatic chromosome arms. Gene. 2003;312:41–50.

Carvalho AB, Clark AG. Y chromosome of *D. pseudoobscura* is not homolog to the ancestral *Drosophila* Y. Science. 2005;307(5706):108–110.

Casale AM, Liguori F, Ansaloni F, Cappucci U, Finaurini S, Spirito G, Persichetti F, Sanges R, Gustincich S, Piacentini L. Transposable element activation promotes neurodegeneration in a *Drosophila* model of Huntington's disease. iScience. 2022;25(1):103702. doi:10.1016/j.isci.2021.103702.

Corradini N, Rossi F, Giordano E, Caizzi R, Vernì F, Dimitri P. *Drosophila melanogaster* as a model for studying protein-encoding genes that are resident in constitutive heterochromatin. Heredity (Edinb). 2007;98(1):3–12.

Cotsworth S, Jackson CJ, Hallson G, Fitzpatrick KA, Syrzycka M, Coulthard AB, Bejsovec A, Marchetti M, Pimpinelli S, Wang SJH, *et al.* Characterization of *Gfat1* (*zeppelin*) and *Gfat2*, essential paralogous genes which encode the enzymes that catalyze the rate-limiting step in the hexosamine biosynthetic pathway in *Drosophila melanogaster*. Cells. 2022;11(3):448.

Crosby MA, Goodman JL, Strelets VB, Zhang P, Gelbart WM; The FlyBase Consortium. Flybase: genomes by the dozen. Nucleic Acids Res. 2007;35(Database):D486–D491. doi:101093/nar/gkl827.

Clark AG, Eisen MB, Smith DR, Bergman CM, Oliver B, Markow TA, Kaufman TC, Kellis M, Gelbart W, Iyer VN, *et al.*; Drosophila 12 Genomes Consortium. Evolution of genes and genomes on the Drosophila phylogeny. Nature. 2007;450(7167):203–218.

Dobzhansky T. Chromosomal races in Drosophila pseudoobscura and Drosophila persimilis. Carnegie Inst Washington Publ. 1944;554:47–144.

Donald HP. On the genetical constitution of *Drosophila pseudo.obscura* race A. J Genet. 1936;33(1):103–122.

Fanti L, Pimpinelli S. Immunostaining of squash preparations of chromosomes of larval brains. Methods Mol Biol. 2004;247:353–361.

Franchini P, Kautt AF, Nater A, Antonini G, Castiglia R, Meyer A, Solano E. Reconstructing the evolutionary history of chromosomal races on islands: a genome-wide analysis of natural house mouse populations. Mol Biol Evol. 2020;37(10):2825–2837.

Fuller ZL, Leonard CJ, Young RE, Schaeffer SW, Phadnis N. Ancestral polymorphisms explain the role of chromosomal inversions in speciation. PLoS Genet. 2018;14(7):e1007526.

Gatti M, Pimpinelli S. Functional elements in *Drosophila melanogaster* heterochromatin. Annu Rev Genet. 1992;26:239–275.

Horvath JE, Schwartz S, Eichler EE. The mosaic structure of human pericentromeric DNA: a strategy for characterizing complex regions of the human genome. Genome Res. 2000;10(6):839–852.

Hoskins RA, Smith CD, Carlson JW, Carvalho AB, Halpern A, Kaminker JS, Kennedy C, Mungall CJ, Sullivan BA, Sutton GG, *et al.* Heterochromatic sequences in a Drosophila whole-genome shotgun assembly. Genome Biol. 2002;3(12):research0085.1.

Hoskins RA, Carlson JW, D Acevedo CK, Evans-Holm M, Frise E, Wan KH, Park S, Mendez-Lago M, Rossi F, Villasante A, *et al.* Sequence finishing and mapping of *Drosophila melanogaster* heterochromatin. Science. 2007;316(5831):1625–1628.

Kuhn RM, Clarke L, Carbon J. Clustered tRNA genes in *Schizosaccharomyces pombe* centromeric DNA sequence repeats. Proc Natl Acad Sci USA. 1991;88(4):1306–1310.

Lemeunier F, Ashburner M. Relationships within the *melanogaster* species subgroup of the genus *Drosophila* (*Sophophora*). II. Phylogenetic relationships between six species based upon polytene chromosome banding sequences. Proc R Soc Lond B Biol Sci. 1976;193(1112):275–294.

Makino T, Kawata M. Habitat variability correlates with duplicate content of Drosophila genomes. Mol Biol Evol. 2012;29(10):3169–3179.

Miller DE, Staber C, Zeitlinger J, Hawley S. Highly contiguous genome assemblies of 15 Drosophila species generated using nanopore sequencing. G3 (Bethesda). 2018;8(10):3131–3141.

Muller HJ. Bearings of the Drosophila work on systematics. In: J Huxley, editor. The New Systematics. Oxford: Clarendon Press; 1940. p. 185–268.

Piacentini L, Fanti L, Specchia V, Bozzetti MP, Berloco M, Palumbo G, Pimpinelli S. Transposons, environmental changes, and heritable induced phenotypic variability. Chromosoma. 2014;123(4):345–354. doi:10.1007/s00412-014–0464-y.

Piacentini L, Marchetti M, Bucciarelli E, Casale AM, Cappucci U, Bonifazi P, Renda F, Fanti L. A role of the Trx-G complex in Cid/CENP-A deposition at *Drosophila melanogaster* centromeres. Chromosoma. 2019;128(4):503–520. doi:10.1007/s00412-019–00711-x.

Pimpinelli S, Gatti M, De Marco A. Evidence for heterogeneity in heterochromatin of *Drosophila melanogaster*. Nature. 1975;256(5515):335–337.

Pimpinelli S, Bonaccorsi S, Fanti L, Gatti M. Preparation and analysis of Drosophila mitotic chromosomes. In: W Sullivan, M Ashburner, RS Hawley, editors. Drosophila Protocols. Cold Spring Harbor (NY): Cold Spring Harbor Laboratory Press; 2000. p. 3–23.

Pimpinelli S, Bonaccorsi S, Fanti L, Gatti M. Chromosome banding of mitotic chromosomes from *Drosophila* larval brain. Cold Spring Harbor Protocols. 2010a;2010:pdb.prot5390. doi:10.1101/pdb.prot5389.

Pimpinelli S, Bonaccorsi S, Fanti L, Gatti M. Fluorescent in situ hybridization (FISH) of mitotic chromosomes from Drosophila larval brain. Cold Spring Harb Protoc. 2010b;2010(3). doi:10.1101/pdb.prot5391.

Pimpinelli S, Bonaccorsi S, Fanti L, Gatti M. Immunostaining of mitotic chromosomes from Drosophila larval brain. Cold Spring

Harb Protoc. 2011;2011(9):pdb.prot065524. doi:10.1101/pdb.prot065524.

Pimpinelli S, Gatti M, De Marco A. Evidence for heterogeneity in heterochromatin of *Drosophila melanogaster*. Nature. 1975;256(5515):335–337.

Ranz JM, Casals F, Ruiz A. How malleable is the eukaryotic genome? Extreme rate of chromosomal rearrangement in the genus Drosophila. Genome Res. 2001;11(2):230–239.

Ruiz A, Fontdevila A. The evolutionary history of *Drosophila buzzatii*. VI. Adaptative chromosomal changes in experimental populations with natural substrates. Genetica. 1985;66(1):63–71.

Sharp-Baker H, Chen RH. Spindle checkpoint protein Bub1 is required for kinetochore localization of Mad1, Mad2, Bub3 and Cenp-E, independently of its kinase activity. J Cell Biol. 2001;153(6):1239–1250.

Segarra C, Aguadè M. Molecular organization of the X chromosome in different species of the *obscura* group of *Drosophila*. Genetics. 1992;130(3):513–521.

Schaeffer SW, Bhutkar A, McAllister BF, Matsuda M, Matzkin LM, O'Grady PM, Rohde C, Valente VLS, Aguadé M, Anderson WW, *et al.* Polytene chromosomal maps of 11 *Drosophila* species: the order of genomic scaffolds inferred from genetic and physical maps. Genetics. 2008;179(3):1601–1655.

Schulze SR, McAllister F, Sinclair DAR, Fitzpatrick KA, Marchetti M, Pimpinelli S, Honda BM. Heterochromatic genes in Drosophila: a comparative analysis of two genes. Genetics. 2006;173(3):1433–1445.

Smith CD, Shu SQ, Mungall CJ, Karpen GH. The release 5.1 annotation of *Drosophila melanogaster* heterochromatin. Science. 2007;316(5831):1586–1591.

Sperlich D, Pfriem P. 1986. Chromosomal polymorphism in natural and experimental populations. In: The Genetics and Biology of Drosophila. M Ashburner, HL Carson, JN Thomson, editors. New York (NY): Academic Press. p. 257–309.

Sturtevant AH, Tan CC. The comparative genetics of *Drosophila pseudoobscura* and *D. melanogaster*. J Genetics. 1937;34(3):415–432.

Sturtevant AH, Novitski E. The homologies of the chromosome elements in the genus *Drosophila*. Genetics. 1941;26(5):517–541.

Vigneron S, Prieto S, Bernis C, Labbè JC, Castro A, Lorca T. Kinetochore localization of spindle checkpoint proteins: who controls whom? Mol Biol Cell. 2004;15(10):4584–4596.

Yogeeswaran K, Frary A, York TL, Amenta A, Lesser AH, Nasrallah JB, Tanksley SD, Nasrallah ME. Comparative genome analyses of *Arabidopsis* spp.: inferring chromosomal rearrangement events in the evolutionary history of *A. thaliana*. Genome Res. 2005;15(4):505–515.

Communicating editor: N. Perrimon